BIOINFORMATICS ORIGINAL PAPER

Vol. 31 no. 3 2015, pages 390–396
doi:10.1093/bioinformatics/btu664

Systems biology

Advance Access publication October 9, 2014

A stochastic automaton model for simulating kinesin processivity

Hamidreza Khataee* and Alan Wee-Chung Liew*

School of Information and Communication Technology, Gold Coast Campus, Griffith University, QLD 4222, Australia

Associate Editor: Alfonso Valencia

ABSTRACT

Motivation: Cellular interactions of kinesin-1, an adenosine triphosphate (ATP)-driven motor protein capable of undergoing multiple steps on a microtubule (MT), affect its mechanical processivity, the number of steps taken per encounter with MT. Even though the processivity of kinesin has been widely studied, a detailed study of the factors that affect the stepping of the motor along MT is still lacking.

Results: We model the cellular interactions of kinesin as a probabilistic timed automaton and use the model to simulate the mechanical processivity of the motor. Theoretical analysis suggests: (i) backward stepping tends to be powered by ATP hydrolysis, rather than ATP synthesis, (ii) backward stepping powered by ATP synthesis is more likely to happen with limiting ATP concentration ([ATP]) at high loads and (iii) with increasing load the frequency of backward stepping powered by ATP hydrolysis at high [ATP] is greater than that powered by ATP synthesis at limiting [ATP]. Together, the higher frequency of backward stepping powered by ATP hydrolysis than by ATP synthesis is found to be a reason for the more dramatic falling of kinesin processivity with rising load at high [ATP] compared with that at low [ATP]. Simulation results further show that the processivity of kinesin can be determined by the number of ATP hydrolysis and synthesis kinetic cycles taken by the motor before becoming inactive. It is also found that the duration of a backward stepping cycle at high loads is more likely to be less than that of a forward stepping cycle.

Contact: h.r.khataee@griffithuni.edu.au or a.liew@griffith.edu.au.

Received on June 7, 2014; revised on September 10, 2014; accepted on October 6, 2014

1 INTRODUCTION

Kinesin-1 is an adenosine triphosphate (ATP)-driven motor protein that walks in an asymmetric hand-over-hand fashion (Yildiz *et al.*, 2004, 2008) on a microtubule (MT) in discrete 8.2 nm steps (Clancy *et al.*, 2011). Mechanical processivity of kinesin has revealed that the motor takes multiple steps in the forward direction (i.e. to the plus end of MT) and occasionally in the backward direction (i.e. to the minus end of MT) (Carter and Cross 2005; Nishiyama *et al.*, 2002; Yildiz *et al.*, 2008) before detaching from MT in the presence of ATP (Howard *et al.*, 1989; Yajima *et al.*, 2002), or in the absence of ATP if external load is applied to the motor (Yildiz *et al.*, 2008). Processivity of kinesin ensures that cellular cargos are transported reliably over long distances. Processive stepping of kinesin exerts localized forces on nanostructures, which can be exploited in nanorobotics by inventing artificial nanomotors and thus, synthetic nanodevices powered by the motor (Fischer *et al.*, 2009; Goodman *et al.*, 2012; Hess 2006). This stepping is also manipulated in the controlled propagation architecture of nanonetworks whose information molecules are carried by kinesin motors between transmitter and receiver nanomachines (Nakano *et al.*, 2012; Pierobon and Akyildiz, 2010). Synthetic nanodevices and nanonetworks are anticipated to contribute in medical diagnostics as well as engineering applications (Fischer *et al.*, 2009; Goodman *et al.*, 2012; Nakano *et al.*, 2012). Despite this progress, artificial nanomotors still lack the functionality and efficiency of their biological counterparts (Wang and Manesh, 2010).

Processivity of kinesin motor and thus, its mean run length (i.e. the distance that the motor travels before detaching from MT) is correlated to the cellular interactions of the motor (Toprak *et al.*, 2009). Yet, little is known about how this motor can remain attached to MT through the hundreds of stepping cycles (Toprak *et al.*, 2009). A better understanding of the cellular interactions of kinesin would provide new insights into the mechanical processivity of the motor. Recently, we developed a mathematical model that simulates the behaviour of kinesin stepping (Khataee and Liew, 2014). We showed that the model could be used to analyse and predict forward and backward stepping of kinesin motor at different ATP concentrations ([ATP]) and loads. On the basis of our findings in Khataee and Liew (2014), here we aim to model the stochastic behaviour of a single kinesin molecule by constructing a probabilistic timed automaton based on a discrete stochastic model of the motor at various [ATP] and loads. The probabilistic timed automata (PTA) are mathematical models augmented with time and discrete probability distributions for modelling the temporal and stochastic properties of stochastic discrete-event systems (Beauquier, 2003; Kwiatkowska *et al.*, 2002, 2004). Our proposed automaton model shows that the mean run length of kinesin, at different [ATP] and loads, can be determined by the number of ATP hydrolysis and synthesis kinetic cycles taken by the motor before detaching from MT.

2 RESULTS

2.1 Theoretical analysis

For a kinesin motor, the four-state discrete stochastic model defines a single stepping cycle as:

$$(1) \underset{w_2}{\overset{u_1}{\leftrightarrow}} (2) \underset{w_3}{\overset{u_2}{\leftrightarrow}} (3) \underset{w_4}{\overset{u_3}{\leftrightarrow}} (4) \underset{w_1}{\overset{u_4}{\leftrightarrow}} (1)$$

$$|\leftarrow d1\rightarrow|\leftarrow d2\rightarrow|\leftarrow d3\rightarrow|\leftarrow d4\rightarrow|$$

*To whom correspondence should be addressed.

Table 1. Estimated parameters in the forward and backward transition rate equations (Fisher and Kolomeisky, 2001)

State i	$u_i^0(s^{-1})$	w_i^0 (s^{-1})	θ_i^+	θ_i^-
1	–	–	0.120	0.430
2	580	40	0.020	0.130
3	290	1.6	0.020	0.130
4	290	40	0.020	0.130

where

$$(1) = \mathrm{M{\cdot}K}, \qquad (2) = \mathrm{M{\cdot}K{\cdot}ATP}$$
$$(3) = \mathrm{M{\cdot}K{\cdot}ADP{\cdot}P_i}, \quad (4) = \mathrm{M{\cdot}K{\cdot}ADP}$$

where M·K denotes MT-kinesin complex and ADP·P_i complex stands for the products of ATP hydrolysis: adenosine diphosphate (ADP) and inorganic phosphate (P_i). The d_i ($i = 1, 2, 3, 4$) represents the substep length for the center of force of kinesin along MT, where the total step size is $d = (d_1 + d_2 + d_3 + d_4)$. In this four-state stochastic model, kinetic state i may transit to states $i + 1$ and $i - 1$ with forward and backward transition rates u_i and w_i ($i = 1, 2, 3, 4$), respectively, influenced by the temperature T and external load F as:

$$u_i^F = u_i^0 \exp\left(-\frac{\theta_i^+ Fd}{k_B T}\right) \tag{1}$$

$$w_i^F = w_i^0 \exp\left(+\frac{\theta_i^- Fd}{k_B T}\right) \tag{2}$$

where u_i^0 and w_i^0 are the transition rates at zero load, θ_i^+ and θ_i^- are the characteristic distances for the load, d is the step size ($= 8.2$ nm) and k_B is the Boltzmann constant (Fisher and Kolomeisky, 2001; Kolomeisky and Fisher, 2007). The load distribution factors demonstrate how the external load affects the individual kinetic rates where it is assumed that $\sum_{i=1}^{4}(\theta_i^+ + \theta_i^-) = 1$. These factors are related to substep lengths via $d_i = (\theta_i^+ + \theta_{i+1}^-)d$ (Kolomeisky and Fisher, 2007). The parameter values of Equations (1) and (2) summarized in Table 1 as well as the parameter values of [ATP]-dependent rates presented in Equations (3) and (4) have been estimated by Fisher and Kolomeisky (2001) through regression on the experimental data of Block and colleagues in (Schnitzer *et al*., 2000; Visscher *et al*., 1999) at room temperature:

$$u_1^0 = k_1[\mathrm{ATP}] \tag{3}$$

$$w_1^0 = \frac{k_1'[\mathrm{ATP}]}{\sqrt[2]{1 + \frac{[\mathrm{ATP}]}{c_1}}} \tag{4}$$

where $k_1 = 1.8\,\mu M^{-1}s^{-1}$, $k'_1 = 0.225\,\mu M^{-1}s^{-1}$, $c_1 = 16\,\mu M$ and no side load has been considered. The discrete stochastic model above asserts that forward stepping of kinesin motor hydrolyses ATP, whereas backward stepping could resynthesize ATP (Fisher and Kim, 2005; Fisher and Kolomeisky, 2001; Kolomeisky and Fisher, 2007). In addition in accordance with several sets of experimental and theoretical findings (Carter and Cross, 2005; Clancy *et al*., 2011; Hackney, 2005; Liepelt and Lipowsky, 2007; Nishiyama *et al*., 2002; Taniguchi *et al*., 2005; Yildiz *et al*., 2008), we recently modelled the probabilities of ATP-driven forward and backward stepping of kinesin using the four-state discrete stochastic model and showed that (Khataee and Liew, 2014): (i) the stall force seems to be almost constant and [ATP]-independent and (ii) backward stepping is related to both ATP hydrolysis and synthesis with rate limiting factor being ATP synthesis. Although forward and backward steppings of kinesin have been observed by Yildiz *et al*. (2008) in the direction of the applied load in the absence of ATP due to the strain on the motor head generated by the load, in this work, we focus on the ATP-driven stepping of kinesin motor based on the four-state discrete stochastic model. [ATP] is considered as a factor that affects the motor velocity at various loads (Schnitzer *et al*., 2000; Visscher *et al*., 1999) and thus, it is proposed as a mean for temporal control of synthetic nanodevices powered by kinesin motor (Dinu *et al*., 2007; Wang and Manesh, 2010).

In modelling kinesin processivity, Block and colleagues in Schnitzer *et al*. (2000) used an energy landscape formalism, where the kinetic rates followed a Boltzmann-type relationship, and showed that the mean run length of kinesin, L, exhibits Michaelis–Menten kinetic behaviour, $L = L_0[\mathrm{ATP}]/([\mathrm{ATP}] + L_M)$, where L_0 is the mean run length at zero load and L_M is Michaelis constant. Using a global analysis of kinesin processivity data carried out from Michaelis–Menten functions at different [ATP] and loads and then, fitted to kinetic rates, L was calculated as follows:

$$L = \frac{8.2 \times [\mathrm{ATP}] \times A\exp\left(-\frac{F\delta}{k_B T}\right)}{[\mathrm{ATP}] + B\left(1 + A\exp\left(-\frac{F\delta}{k_B T}\right)\right)} \tag{5}$$

where $A = 107 \pm 9$ gives the maximum average number of catalytic cycles before detachment, $\delta = 1.3 \pm 0.1$ nm is the characteristic distance associated with load dependence and $B = 0.029 \pm 0.009\,\mu M$ is a parameter of Michaelis constant. It was observed that run lengths of kinesin motor are exponentially distributed under fixed load or [ATP] (Schnitzer *et al*., 2000; Yajima *et al*., 2002). The energy landscape model proposed in Schnitzer *et al*. (2000) predicts that kinesin motility should remain tightly coupled to ATP hydrolysis even under load. Meanwhile, the four-state discrete stochastic model, derived from this energy model, describes the dynamics of kinesin stepping by both the ATP hydrolysis and synthesis kinetic cycles at various [ATP] and loads (Fisher and Kolomeisky, 2001; Kolomeisky and Fisher, 2007). Even though Carter and Cross (2005) stated that backward stepping is unlikely to result in ATP synthesis, Fisher and Kim (2005) remarked that the experimental observations in Carter and Cross (2005) rest on a misconception of the significance of dwell times before forward and backward stepping, and asserted that backward stepping could actually result in ATP synthesis.

The four-state discrete stochastic model and our modelling of mechanical kinetics of kinesin stepping in Khataee and Liew (2014) allow us to simulate the processivity of kinesin motor by considering both the ATP hydrolysis and synthesis kinetic cycles at various [ATP] and loads. The four-state discrete

stochastic model can be used to count the net number of steps taken by the motor before becoming inactive. Therefore, we simulate the processivity of kinesin by computing the number of ATP hydrolysis and synthesis kinetic cycles and thus, the mean number of steps taken by the motor before detachment from MT at different settings of [ATP] and load. It has been shown that there is a small probability of detachment per mechanical stepping cycle (Block *et al.*, 1990; Schliwa, 2003). As the detachment of kinesin from MT in each stepping cycle is an independent event and does not depend on any previous stepping cycles, the distribution of the number of steppings before detaching of kinesin from MT is a geometric distribution. Thus, the mean number of forward steps derived from ATP hydrolysis before the motor becomes inactivated is given by:

$$\langle n_h \rangle = \frac{1}{P_{off}} \tag{6}$$

where P_{off} is the detachment probability of kinesin from MT per mechanical stepping cycle. Since kinesin dissociates from MT after each single run, the detachment probability of the motor from MT per mechanical stepping cycle in relation with the mean run length is exponentially distributed as follows (Yajima *et al.*, 2002):

$$P_{off} = \left(1 - \exp\left(-\frac{8.2}{L}\right)\right) \tag{7}$$

where L is the mean run length given by Equation (5). To obtain the mean number of steps taken by kinesin per encounter with MT, the mean number of backward steps derived from ATP synthesis should be deducted from $<n_h>$. We define the mean number of backward steps derived from ATP synthesis before detaching of kinesin from MT as follows:

$$\langle n_s \rangle = \langle n_h \rangle \times P_s \tag{8}$$

where P_s is the proportion of ATP synthesis pathway to ATP hydrolysis pathway defined as follows:

$$P_s = \frac{w_3^F}{u_2^F + w_3^F} \tag{9}$$

where u_2^F and w_3^F are computed by Equations (1) and (2). Thus, the mean number of steps taken by kinesin per encounter with MT is defined as follows:

$$\langle n \rangle = \langle n_h \rangle - \langle n_s \rangle \tag{10}$$

Theoretical predictions for the processivity of kinesin motor at different [ATP] and loads are obtained from Equation (10) (Fig. 1). Figure 1A and B shows that the processivity of kinesin motor dramatically declines with increasing load or decreasing [ATP], in agreement with previous findings in Liepelt and Lipowsky (2007) and Schnitzer *et al.* (2000). Experimental data in Schnitzer *et al.* (2000) showed that at low loads and high [ATP], the mean run length L was ~600 nm. L fell to ~300 nm when the [ATP] was reduced to 5 μM, and to ~80 nm when load was increased to 5 pN. We show that the computed $<RL>$ is comparable with the experimentally obtained L, where $<RL>$ is almost equal to: ~601 nm at [ATP] = 1 mM and F = 1.1 pN, ~300 nm at [ATP] = 5 µM and F = 2.4 pN and ~80 nm when

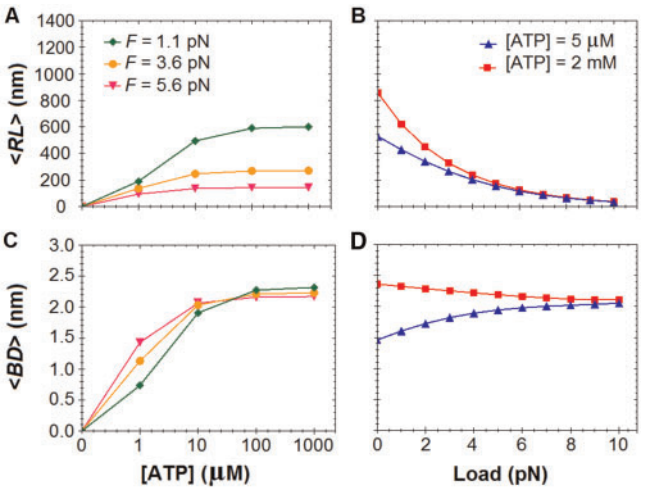

Fig. 1. Mean run length ($<RL>$) and mean backward displacement powered by ATP synthesis ($<BD>$). $<RL>$, calculated as $<n> \times 8.2$ nm [Equation (10)], as a function of (**A**) [ATP] at various loads and (**B**) load F at different [ATP]. $<BD>$ calculated as $<n_s> \times 8.2$ nm [Equation (8)] against (**C**) [ATP] at different loads and (**D**) load F at various [ATP]

load increases to 5 pN at [ATP] ~1 µM. Results in Fig. 1A and B also agree with the findings of Liepelt and Lipowsky (2007) in which a 7-state kinetic scheme, based on several motor cycles, was used to calculate the $<RL>$.

At high [ATP], Figure 1C and D indicates that the mean backward displacement ($<BD>$) powered by ATP synthesis decreases with rising load. This implies that the falling of $<RL>$ with rising load at high [ATP] observed in Figure 1B could only be due to the rising frequency of backward stepping powered by ATP hydrolysis. This is in agreement with the experimental observations in Carter and Cross (2005) and Nishiyama *et al.* (2002) and theoretical results in Khataee and Liew (2014) and Liepelt and Lipowsky (2007) that backward steppings are mainly generated by ATP hydrolysis at high [ATP]. At limiting [ATP], backward stepping powered by ATP hydrolysis has low frequency due to low [ATP]. At low [ATP], Figure 1D shows that $<BD>$ has rising trend, indicating that ATP is increasingly likely to be synthesized during backward movement, as reported in Fisher and Kim (2005), Fisher and Kolomeisky (2001) and Kolomeisky and Fisher (2007). However, the slower falling rate of $<RL>$ at limiting [ATP] than at high [ATP] in Figure 1B indicates that the rate of backward stepping powered by ATP synthesis at limiting [ATP] is lower than the rate of backward stepping powered by ATP hydrolysis at high [ATP]. This supports the observations that backward steppings are more likely to be generated by ATP hydrolysis than by ATP synthesis when [ATP] is not limiting, and that the frequency of backward stepping rises with [ATP] (Carter and Cross, 2005). Moreover, Figure 1C shows that the rise of $<BD>$ slows down with increasing [ATP], implying that backward stepping powered by ATP synthesis is more likely to happen with limiting [ATP]. Together, these theoretical analyses indicate that

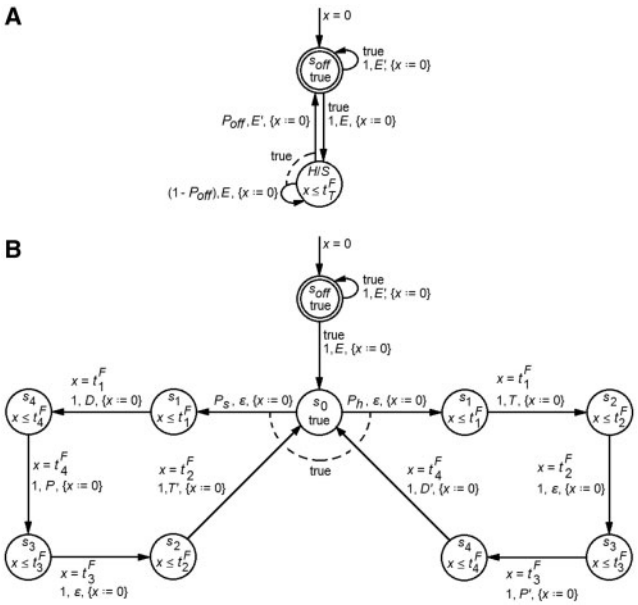

Fig. 2. The automaton model, M_{kinesin}. (**A**) General representation of M_{kinesin}. M_{kinesin} starts with incoming unlabeled arrow to state s_{off} with clock x initialized to 0. As the invariant condition of s_{off} is true, the control stays in state s_{off} until perceiving input E. By sensing input E, s_{off} changes to state H/S and clock x is reset to 0. In state H/S, one of ATP hydrolysis or synthesis pathway is randomly chosen to run or M_{kinesin} becomes inactivated with probability P_{off}. (**B**) Detailed representation of M_{kinesin}. By sensing input E, ATP hydrolysis or synthesis pathway is chosen to run with probability P_h or P_s, respectively. Then, the value of clock x increases uniformly with time. When x is equal to t_1^F the invariant condition $x \leq t_1^F$ requires that the action with event T or D must be taken. Alternatively, if x exceeds t_1^F then the action with event label $\acute{E}$ may be taken with probability 1. These behaviours correspond to the attachment of kinesin to MT in the absence of regulatory factors and the start of stepping initiated with kinetic state changing $1 \xrightarrow{u_1} 2$ or $1 \xrightarrow{w_1} 4$. However, if [ATP] is limiting then the motor detaches from MT due to long pausing. For clarity of the graph, transitions of a single action are connected with a dotted line. Also, actions a_{i3} ($i = 1, 2, 3, 4$) are not shown

the processivity of kinesin can be determined by the number of ATP hydrolysis and synthesis kinetic cycles taken by the motor before becoming inactive.

2.2 Automaton model

To simulate how the cellular interactions of kinesin affect its processivity, we abstract an important set of its cellular interactions as a parametric probabilistic timed automaton (Alur and Dill, 1994; Alur *et al.*, 1993; Beauquier, 2003; Kwiatkowska *et al.*, 2002, 2004; Sproston and Troina, 2010), and construct the automaton model shown in Figure 2 with $M_{\text{kinesin}} = (S, s_{\text{initial}}, s_{\text{final}}, I, C, tran, inv, A_s, EC_s)$. The model simulates the ATP hydrolysis and synthesis kinetic pathways that resulted in the processivity of kinesin at various [ATP] and loads. The set $S = \{s_{\text{off}}, H/S\}$ in Figure 2A denotes the states of M_{kinesin} where s_{off} corresponds to the kinetic state in which kinesin is detached from MT and state H/S stand for an ATP hydrolysis (H) or synthesis (S) kinetic cycle. State H/S is composed of H and S cycles connected by a state s_0 defined to determine which cycle is randomly chosen to be executed. Each H or S cycle is composed of states s_1–s_4, which stand for the kinetic states '1'–'4' of the four-state discrete stochastic model, respectively (Fig. 2B). $s_{\text{initial}} = \{s_{\text{off}}\} \subset S$ and $s_{\text{final}} = \{s_{\text{off}}\} \subset S$ are the initial and final states of M_{kinesin}, respectively, because, *in vivo*, kinesin mainly exists as soluble motor where its activity is switched off and the motor is autoinhibited from binding to and moving on MTs (Kaan *et al.*, 2011; Verhey and Rapoport, 2001). The input set $I = \{E, T, D, P, E', T', D', P'\}$ denotes the events E, T, D and P, which stand for the presence of enabling condition of kinesin (e.g. low external loads, the presence of MT and the absence of regulatory factors), ATP binding, ADP binding and P_i binding, respectively. The complement of an event (i.e. E', T', D' or P') represents the opposite molecular role of that event. To express the temporal properties of kinesin mechanism, we define the clock set $C = \{x\}$, which contains a non-negative real-valued variable (i.e. $\in \mathrm{R}^+$) that increases at the same rate as real time. Clock x indicates the time elapsed in M_{kinesin} states, corresponding to the mean waiting time in kinetic states of kinesin. The set $tran$ of transitions which are tuples of the form $e_s = (s, p, a, \check{C}, s')$ representing a transition from state s to state s' with probability p, event $a \in I \cup \{\varepsilon\}$ and set $\check{C} \subseteq C$ of clocks which are reset to 0 by transition e_s, where ε denotes null event. The function inv: $S \rightarrow \zeta$ is defined to assign to each state of M_{kinesin} an invariant condition from the set ζ of clock constraints. A state stays invariant, i.e., no change, when the constraint is true. The invariant condition of state s_{off} is assigned as true because, *in vivo,* kinesin mainly stays in the detached state without time constraint. As state s_0 is defined to determine the kinetic pathway, its invariant condition is assigned as true to show no time constraint. For states s_1–s_4, we assign invariant conditions $x \leq t_i^F$ where clock $x \in C$ and t_i^F denotes the mean wait time of kinesin in kinetic states i ($i = 1, 2, 3, 4$). It was shown that the waiting time in each kinetic state is inversely proportional to the transition rate from that state (Leibler and Huse, 1993). Therefore, t_i^F is calculated as follows:

$$t_i^F = \frac{1}{u_i^F + w_i^F} \tag{11}$$

where the transition rates u_i^F and w_i^F are computed using Equations (1) and (2) and $i = 1, 2, 3, 4$ (Khataee and Liew, 2014). The invariant condition of state H/S in Figure 2A is defined as the H or S cycle completion time as follows:

$$t_T^F = \sum_{i=1}^{4} t_i^F \tag{12}$$

where t_i^F is given by Equation (11). To associate a non-empty set of finite discrete probability distributions with each state s_i ($i = \text{off}, 0, 1, 2, 3, 4$), we define action sets $A_i = \{a_{i1}, \ldots, a_{ij}\}$ such that:

$$\sum_{e_i \in \text{tran}} p(a_{ij}, e_i) = 1 \tag{13}$$

where $p(a_{ij}, e_i)$ is the probability of using the edge e_i from source state s_i if the action j has been chosen and j is the number of actions associated with state s_i. Two actions $a_{\text{off}1}$ and $a_{\text{off}2}$ are

associated with state s_{off}, i.e. $A_{off} = \{a_{off1}, a_{off2}\}$, representing staying in detached state of kinesin and the attachment of kinesin to MT, respectively. For transitions from state s_0 to the ATP hydrolysis or synthesis pathway, a single action a_{01} is assigned to define the proportion of each pathway with probability P_s given by Equation (9) and P_h given as follows:

$$P_h = \frac{u_2^F}{u_2^F + w_3^F} \tag{14}$$

where u_2^F and w_3^F are computed by Equations (1) and (2). Three actions are associated with each state s_i (i = 1, 2, 3, 4), i.e. $A_i = \{a_{i1}, a_{i2}, a_{i3}\}$: a_{i1} and a_{i2} correspond to the forward and backward kinetic transitions from kinetic state i and a_{i3} expresses the detachment of kinesin from MT in kinetic state i or staying in kinetic state i. To compute the probability of actions a_{i3}, we distribute P_{off} given by Equation (7) to states s_1–s_4 according to the probability of being in each state. Therefore, the inactivation probabilities of $M_{kinesin}$ in states s_1–s_4 per H or S cycle, corresponding to the detachment probabilities of kinesin from MT in kinetic states i (i = 1, 2, 3, 4) per mechanical cycle, are defined as follows:

$$P_{off}(s_i) = P_{off} \times P_i \tag{15}$$

where P_i is the probability in kinetic states i defined as follows (Khataee and Liew, 2014):

$$P_i = \frac{\sum_i}{\sum_T} \tag{16}$$

where

$$\sum\nolimits_1 = w_2^F w_3^F w_4^F + u_2^F u_3^F u_4^F + u_3^F u_4^F w_2^F + u_4^F w_3^F w_2^F \tag{17}$$

$$\sum\nolimits_2 = u_1^F w_4^F w_3^F + w_1^F w_4^F w_3^F + u_1^F u_3^F u_4^F + u_4^F u_1^F w_3^F \tag{18}$$

$$\sum\nolimits_3 = u_1^F u_2^F w_4^F + u_4^F u_1^F u_2^F + w_2^F w_1^F w_4^F + u_2^F w_1^F w_4^F \tag{19}$$

$$\sum\nolimits_4 = u_1^F u_2^F u_3^F + w_1^F w_2^F w_3^F + u_3^F w_2^F w_1^F + u_2^F u_3^F w_1^F \tag{20}$$

$$\sum\nolimits_T = \sum\nolimits_1 + \sum\nolimits_2 + \sum\nolimits_3 + \sum\nolimits_4 \tag{21}$$

Finally, the function EC_i: $a_{ij} \rightarrow \zeta$ is defined to assign an enabling condition to each action $a_{ij} \in A_i$, where i = off, 0, 1, 2, 3, 4 and j is the number of actions associated with state s_i. An enabling condition allows the corresponding action to be triggered. The enabling condition of actions associated with state s_{off} is assigned as true, EC_{off}: a_{off1}, $a_{off2} \rightarrow$ true, meaning that these actions can be triggered at any time. This resembles the cellular mechanism of kinesin, which can stay unattached or attached to MT without time constraint. The enabling condition of action a_{01} associated with state s_0 is also assigned as true, i.e. EC_0: $a_{01} \rightarrow$ true, meaning that upon the attachment of kinesin to MT, ATP hydrolysis or synthesis pathway can be taken randomly without time constraint. The enabling conditions of actions associated with states s_1–s_4 and resemble forward or backward kinetic transition are assigned as $x = t_i^F$, where $x \in C$ and t_i^F is computed using Equation (11). These conditions enable transitions to be triggered when the mean wait times in their corresponding states are met. For the third actions of states s_1–s_4, a_{i3} (i = 1, 2, 3, 4), the enabling condition is assigned as true, meaning that the detachment of kinesin from MT in kinetic state i or staying in kinetic state i has no time constraint.

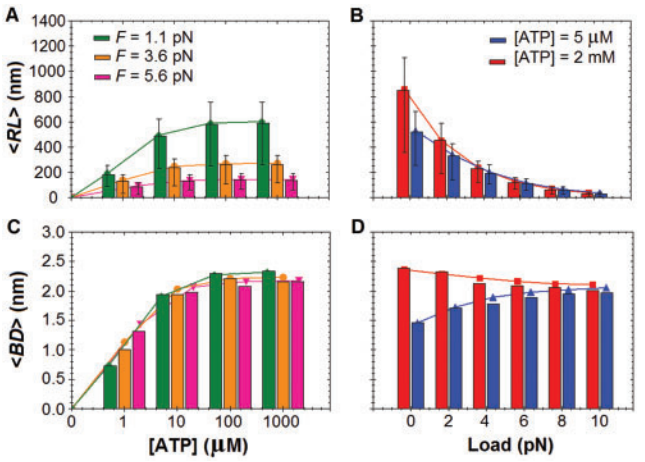

Fig. 3. Stochastic simulation of <*RL*> and <*BD*>. Simulation results are shown by bar graphs. Line graphs are the results obtained from theoretical analysis, as shown in Figure 1. $M_{kinesin}$ simulates <*RL*> as a function of (**A**) [ATP] at various loads and (**B**) load F at different [ATP]. $M_{kinesin}$ also simulates <*BD*>, computed by the mean number of $T(s)$ traces × 8.2 nm, against (**C**) [ATP] at different loads and (**D**) load F at various [ATP]. The 25 and 75 percentile values obtained from the simulation are shown in A and B panels. For panels C and D, these values are equal to zero showing that more than 75% of runs of $M_{kinesin}$ do not execute $T(s)$ trace

2.3 Simulations and discussion

To simulate the processivity of kinesin using $M_{kinesin}$ model at various [ATP] and loads, the function of $M_{kinesin}$ is analysed over its states, according to the principles of PTA, where the behaviour of a system is modelled as a sequence of system states (or events) called a trace (Alur and Dill, 1994). Accordingly, to simulate the processivity of kinesin, we compute the numbers of the following two traces completed in each run of $M_{kinesin}$:

$$T(h)\text{: } s_0 \rightarrow s_1 \rightarrow s_2 \rightarrow s_3 \rightarrow s_4 \rightarrow s_0$$

$$T(s)\text{: } s_0 \rightarrow s_1 \rightarrow s_4 \rightarrow s_3 \rightarrow s_2 \rightarrow s_0$$

where $T(h)$ and $T(s)$ traces correspond to the stepping cycle derived from ATP hydrolysis and synthesis kinetic cycle, respectively. In each run, $M_{kinesin}$ starts in state s_{off}, transits stochastically between H or S cycles by executing $T(h)$ and $T(s)$ traces until it becomes randomly inactivated in state s_{off}. This run corresponds to the attachment of kinesin to MT, hydrolysis or synthesis of ATP, and detachment from MT. Hence, the mean numbers of $T(h)$ and $T(s)$ traces after many runs of $M_{kinesin}$ would represent $<n_h>$ and $< n_s>$, respectively. Then, using Equation (10), <*RL*> is computed by

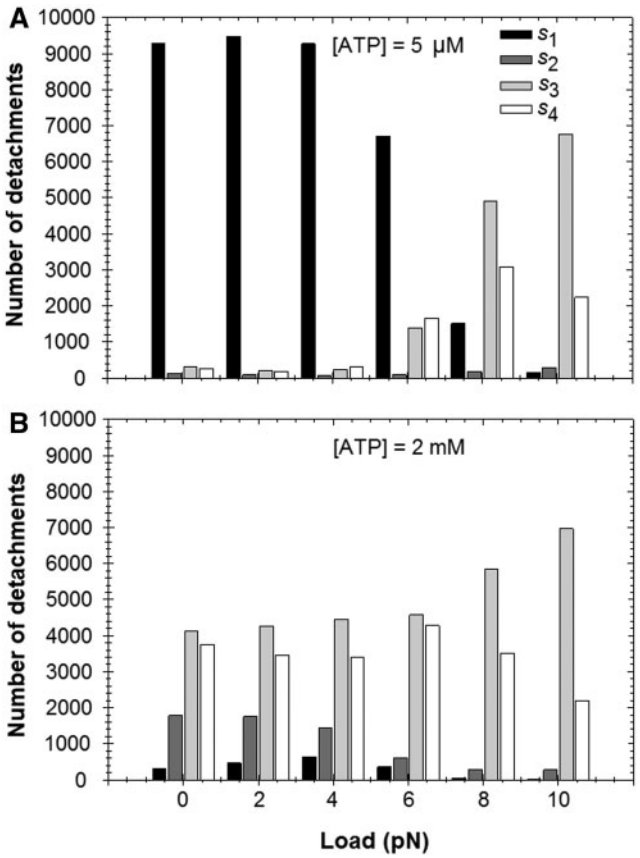

Fig. 4. The number of M_{kinesin} inactivations in states s_1–s_4, corresponding to the number of detachments of kinesin from MT in each kinetic state '1'–'4', versus load at different [ATP]

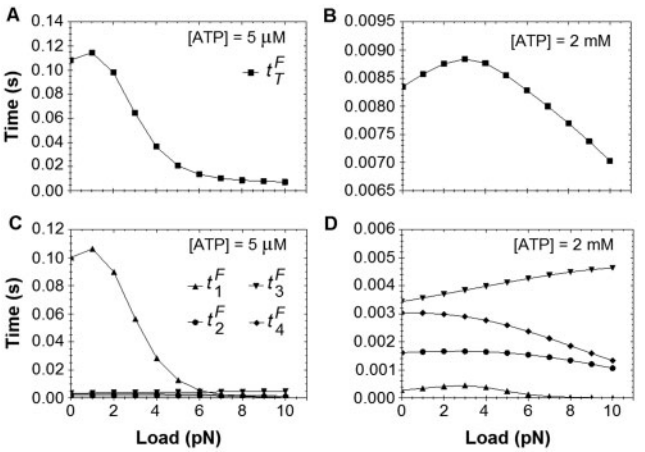

Fig. 5. Duration of a single cycle of M_{kinesin} and durations of states s_1–s_4. (**A** and **B**) Duration of a single cycle of M_{kinesin} calculated by Equation (12) and corresponding to the cycle completion time of kinesin stepping. (**C** and **D**) Durations of states s_1– of M_{kinesin} are calculated by Equation (11) and correspond to the mean waiting time in kinetic states '1'–'4' (Khataee and Liew, 2014)

$<n> \times 8.2$ nm. M_{kinesin} is run for 10 000 times and the simulation results of $<RL>$, shown in Figure 3A and B, indicate good agreement with experimental observations in Schnitzer *et al.* (2000) and theoretical findings in Liepelt and Lipowsky (2007). Results in Figure 3A and B show that the processivity of kinesin diminishes with increasing load or decreasing [ATP], as showed in Liepelt and Lipowsky (2007) and Schnitzer *et al.* (2000). Similar to Figure 1C and D, simulation results in Figure 3C and D show that $<BD>$ is less than 8.2 nm, implying that on average kinesin is not likely to step backward by synthesizing ATP. This supports the observations that backward steppings are more likely to be generated by ATP hydrolysis (Carter and Cross, 2005). The low $<BD>$ is due to the low rate of ATP synthesis, w_3^F, compared with that of ATP hydrolysis, u_2^F, which leads to low P_s in comparison with P_h. Therefore, the mean number of $T(s)$ trace is below 1. This low mean number of $T(s)$ trace indicates that very few $T(s)$ traces are executed by M_{kinesin}, supporting the theory of the four-state discrete stochastic model in Fisher and Kim (2005), Fisher and Kolomeisky (2001) and Kolomeisky and Fisher (2007) that backward stepping could result in ATP synthesis. Figure 3A–D also indicates a close agreement between the simulation results and the results obtained from theoretical analysis. This agreement of our simulation and theoretical results indicates that the number of $T(h)$ and $T(s)$ traces executed by M_{kinesin} can be used to determine the mean run length of kinesin.

Temporal analysis of M_{kinesin} shown in Figure 4 indicates that the inactivation of M_{kinesin} executing either the $T(h)$ or $T(s)$ trace most probably occurs: (i) in state s_1 at low [ATP] and low loads and (ii) in states s_3 and s_4 at high loads or high [ATP]. These analyses suggest kinetic state '1' to be the most probable kinetic state for kinesin detachment from MT at low [ATP] and low loads (Fig. 4A). This is consistent with the detachment of kinesin from MT due to a long mean waiting time in kinetic state '1' at limiting [ATP], as observed experimentally in Schnitzer *et al.* (2000) and shown theoretically in Khataee and Liew (2014). In accordance with the findings of Schnitzer *et al.* (2000) that at high [ATP] the probability of detachment from kinetic state '1' diminishes, our simulation further shows that at high [ATP] kinetic states '3' and '4' are the first and second most probable kinetic states for the detachment of kinesin from MT due to their longer durations (Fig. 4B). This is in agreement with the reported kinetic states for the detachment of kinesin from MT (Khataee and Liew, 2014; Schliwa, 2003; Seitz and Surrey, 2006). These results are also consistent with the weak affinity of kinesin to MT in kinetic states '3' and '4' (Schliwa, 2003; Seitz and Surrey, 2006). Simulation results in Figure 4 further confirm the small detachment probability of kinesin from MT in kinetic state '2', as reported in Seitz and Surrey (2006) due to tight affinity of the motor to MT in this state. In analyzing the temporal properties of M_{kinesin}, Equation (12) further indicates that at low [ATP] and low loads the duration of a stepping cycle is dominated by the duration of kinetic state '1' due to waiting for ATP binding (Fig. 5), as reported in Schnitzer *et al.* (2000). With increasing load, t_T^F curve decreases suggesting that the duration of a backward stepping cycle at high loads is more likely to be less than that of a forward stepping cycle. In discussing the durations of kinetic states, it was shown that with an increase in the

rate of ATP synthesis at high loads, the detachment probability of kinesin from MT would decrease as the duration of being in kinetic state '3' diminishes (Khataee and Liew, 2014). Hence, the rise of ATP synthesis rate would lead to a rise in the backward stepping frequency and thus, lowering $<RL>$.

In conclusion, our probabilistic timed automaton model constructed using the simple four-state discrete stochastic model could accurately simulate the mechanical processivity of a single kinesin motor at various [ATP] and loads. We showed that the mean run length of the motor can be calculated by considering both the ATP hydrolysis and synthesis kinetic cycles. By simulating both the ATP hydrolysis and synthesis kinetic pathways, we could also explain some of the discrepancies between the previously reported theoretical and experimental findings.

ACKNOWLEDGEMENTS

This work was supported by the International Postgraduate Research Scholarship (IPRS) and the Australian Postgraduate Award (APA) of Griffith University.

Conflict of Interest: none declared.

REFERENCES

Alur,R. and Dill,D.L. (1994) A theory of timed automata. *Theor. Comput. Sci.*, **126**, 183–235.

Alur,R., Henzinger,T.A. and Vardi,M.Y. (1993) Parametric real-time reasoning. In: *Proc. 25th Ann. ACM Symp. on Theory of Comput (STOC)*. ACM, pp. 592–601.

Beauquier,D. (2003) On probabilistic timed automata. *Theor. Comput. Sci.*, **292**, 65–84.

Block,S.M. *et al.* (1990) Bead movement by single kinesin molecules studied with optical tweezers. *Nature*, **348**, 348–352.

Carter,N.J. and Cross,R.A. (2005) Mechanics of the kinesin step. *Nature*, **435**, 308–312.

Clancy,B.E. *et al.* (2011) A universal pathway for kinesin stepping. *Nat. Struct. Mol. Biol.*, **18**, 1020–1027.

Dinu,C.Z. *et al.* (2007) Cellular motors for molecular manufacturing. *Anat. Record*, **290**, 1203–1212.

Fischer,T., Agarwal,A. and Hess,H. (2009) A smart dust biosensor powered by kinesin motors. *Nature Nanotechnol.*, **4**, 162–166.

Fisher,M.E. and Kim,Y.C. (2005) Kinesin crouches to sprint but resists pushing. *Proc. Natl Acad. Sci. USA*, **102**, 16209–16214.

Fisher,M.E. and Kolomeisky,A.B. (2001) Simple mechanochemistry describes the dynamics of kinesin molecules, *Proc. Natl Acad. Sci. USA*, **98**, 7748–7753.

Goodman,B.S., Derr,N.D. and Reck-Peterson,S.L. (2012) Engineered, harnessed, and hijacked: synthetic uses for cytoskeletal systems. *Trends. Cell. Biol.*, **22**, 644–652.

Hackney,D.D. (2005) The tethered motor domain of a kinesin-microtubule complex catalyzes reversible synthesis of bound ATP. *Proc. Natl Acad. Sci. USA*, **102**, 18338–18343.

Hess,H. (2006) Toward devices powered by biomolecular motors. *Science*, **312**, 860–861.

Howard,J., Hudspeth,A.J. and Vale,R.D. (1989) Movement of microtubules by single kinesin molecules. *Nature*, **342**, 154–158.

Kaan,H.Y.K., Hackney,D.D. and Kozielski,F. (2011) The structure of the kinesin-1 motor-tail complex reveals the mechanism of autoinhibition. *Science*, **333**, 883–885.

Khataee,H. and Liew,A.W.C. (2014) A mathematical model describing the mechanical kinetics of kinesin stepping. *Bioinformatics*, **30**, 353–359.

Kolomeisky,A.B. and Fisher,M.E. (2007) Molecular motors: a theorist's perspective. *Annu. Rev. Phys. Chem.*, **58**, 675–695.

Kwiatkowska,M. *et al.* (2002) Automatic verification of real-time systems with discrete probability distributions. *Theor. Comput. Sci.*, **282**, 101–150.

Kwiatkowska,M. *et al.* (2004) Symbolic model checking for probabilistic timed automata. *Lect. Notes Comput. Sci.*, **3253**, 293–308.

Leibler,S. and Huse,D.A. (1993) Porters versus rowers: a unified stochastic model of motor proteins. *J. Cell Biol.*, **121**, 1357–1368.

Liepelt,S. and Lipowsky,R. (2007) Kinesin's network of chemomechanical motor cycles. *Phys. Rev. Lett.*, **98**, 2581021–2581024.

Nakano,T. *et al.* (2012) Molecular communication and networking: Opportunities and challenges. *IEEE Trans. Nanobiosci.*, **11**, 135–148.

Nishiyama,M., Higuchi,H. and Yanagida,T. (2002) Chemomechanical coupling of the forward and backward steps of single kinesin molecules. *Nat. Cell Biol.*, **4**, 790–797.

Pierobon,M. and Akyildiz,I.F. (2010) A physical end-to-end model for molecular communication in nanonetworks. *IEEE J. Sel. Area. Commun.*, **28**, 602–611.

Schliwa,M. (2003) *Molecular Motors*. Wiley-VCH, Weinheim, Germany, pp. 253–257.

Schnitzer,M.J., Visscher,K. and Block,S.M. (2000) Force production by single kinesin motors. *Nat. Cell Biol.*, **2**, 718–723.

Seitz,A. and Surrey,T. (2006) Processive movement of single kinesins on crowded microtubules visualized using quantum dots. *EMBO J.*, **25**, 267–277.

Sproston,J. and Troina,A. (2010) Simulation and bisimulation for probabilistic timed automata. *Lect. Notes Comput. Sci.*, **6246**, 213–227.

Taniguchi,Y. *et al.* (2005) Entropy rectifies the Brownian steps of kinesin. *Nat. Chem. Biol.*, **1**, 342–347.

Toprak,E. *et al.* (2009) Why kinesin is so processive. *Proc. Natl Acad. Sci. USA*, **106**, 12717–12722.

Verhey,K.J. and Rapoport,T.A. (2001) Kinesin carries the signal. *Trends. Biochem. Sci*, **26**, 545–550.

Visscher,K., Schnltzer,M.J. and Block,S.M. (1999) Single kinesin molecules studied with a molecular force clamp. *Nature*, **400**, 184–189.

Wang,J. and Manesh,K.M. (2010) Motion control at the nanoscale. *Small*, **6**, 338–345.

Yajima,J. *et al.* (2002) Direct long-term observation of kinesin processivity at low load. *Curr. Biol.*, **12**, 301–306.

Yildiz,A. *et al.* (2008) Intramolecular strain coordinates kinesin stepping behaviour along microtubules. *Cell*, **134**, 1030–1041.

Yildiz,A. *et al.* (2004) Kinesin walks hand-over-hand. *Science*, **303**, 676–678.